SEASONAL VARIATIONS OF COASTAL CURRENTS OFF THE OREGON - NORTHERN CALIFORNIA COAST

William Frederick Whitson

NAVAL POSTGRADUATE SCHOOL
Monterey, California

THESIS

SEASONAL VARIATIONS OF COASTAL CURRENTS
OFF THE
OREGON - NORTHERN CALIFORNIA COAST

by

William Frederick Whitson

Thesis Advisor: Robert H. Bourke

June 1972

Approved for public release; distribution unlimited.

T147648

Seasonal Variations of Coastal Currents off the Oregon - Northern California Coast

by

William Frederick Whitson
Ensign, United States Navy
B.S., Auburn University, 1971

Submitted in partial fulfillment of the
requirements for the degree of

MASTER OF SCIENCE IN OCEANOGRAPHY

from the

NAVAL POSTGRADUATE SCHOOL

June 1972

ABSTRACT

Seasonal longshore flow patterns are examined at four points along the Oregon-Northern California coast. Summer and winter activity is examined as far seaward as 25 nautical miles and as deep as 200 meters. Long-term mean hydrographic data are used to determine geostrophic velocities. A nearshore baroclinic southward flow (~20 cm/sec) is observed at each of the points during the summer. Winter currents are generally very small (<10 cm/sec) and largely barotropic in nature. Seasonal volume transports are presented; corrected velocity profiles are also presented based on data from moored current meters. Qualitative explanations of the observed phenomena are considered.

TABLE OF CONTENTS

LIST OF TABLES

LIST OF FIGURES

LIST OF FIGURES (continued)

ACKNOWLEDGEMENTS

I wish to extend sincere thanks to Dr. Robert H. Bourke for his guidance in this endeavor. He was constantly available for discussion and explanation and helped me through the numerous crises inherent in the evolution of a thesis.

Dr. Jerry A. Galt provided a great deal of insight into the topic and served as a critical reader of the manuscript. His assistance and suggestions are valued and appreciated.

I wish to extend thanks to Dr. C. N. K. Mooers of the Rosenstiel School of Marine and Atmospheric Science who graciously provided a pre-print of the article he has co-authored with Drs. C. A. Collins and R. L. Smith.

I also wish to thank LT Byron L. Kolitz who contributed greatly to my understanding of oceanographic dynamics. His skillful classroom presentations decreased the amount of necessary background reading and hastened completion of this work.

To my wife I extend special thanks for her patience with and assistance in the preparation of this thesis.

I. INTRODUCTION

A. DESCRIPTION OF AREA OF STUDY

The area of the study, shown in Figure 1, is the one studied by Bourke (1971). More specifically it is bounded by 41° and 46° North latitude. It extends from the coast of Oregon out to approximately 25 nautical miles. Subsurface activity is examined down to a depth of 200 meters.

The California Current flows through the study area and is the main influence on water movement. Significant variations from the California Current pattern may develop locally. These deviations may be attributed to winds, tides, the shallow topography or a combination of these elements.

The topography is characteristic of the West Coast of the United States in that the shelf is very narrow and steep. Steepness generally increases southward as seen in Figure 2. Immediately north of Zone A is Astoria Canyon just off the mouth of the Columbia River. At the southern end of Zone B are located Heceta Bank and Stonewall Bank, features that shoal to depths less than 60 meters and may cause some deflection of the longshore current. The protrusion just south of Heceta Bank is Cape Blanco which divides Zone C from Zone D.

A mixture of the Oyashio and the Kuroshio current systems supplies the California Current. The current is broad, slow, and shallow (~500 m). It flows southward in a band roughly 300 miles wide at an average speed of 10 cm/sec (Dodimead, Favorite, and Hirano, 1963). A seasonal variation of the California Current is the Davidson Current. It develops off the Washington-Oregon coast in September, becomes well

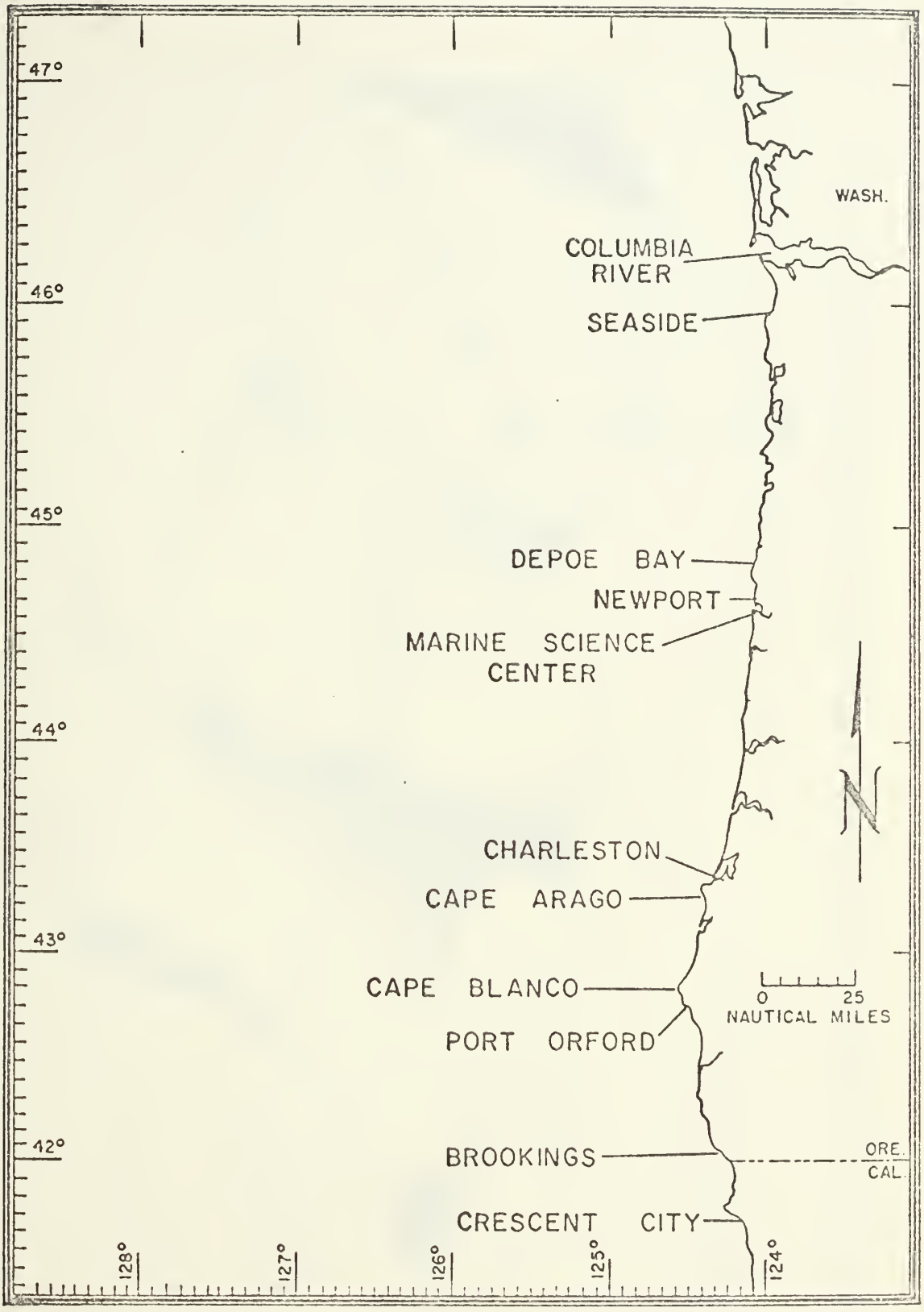

Figure 1. The coastal boundary of the study area. (from Bourke, 1971)

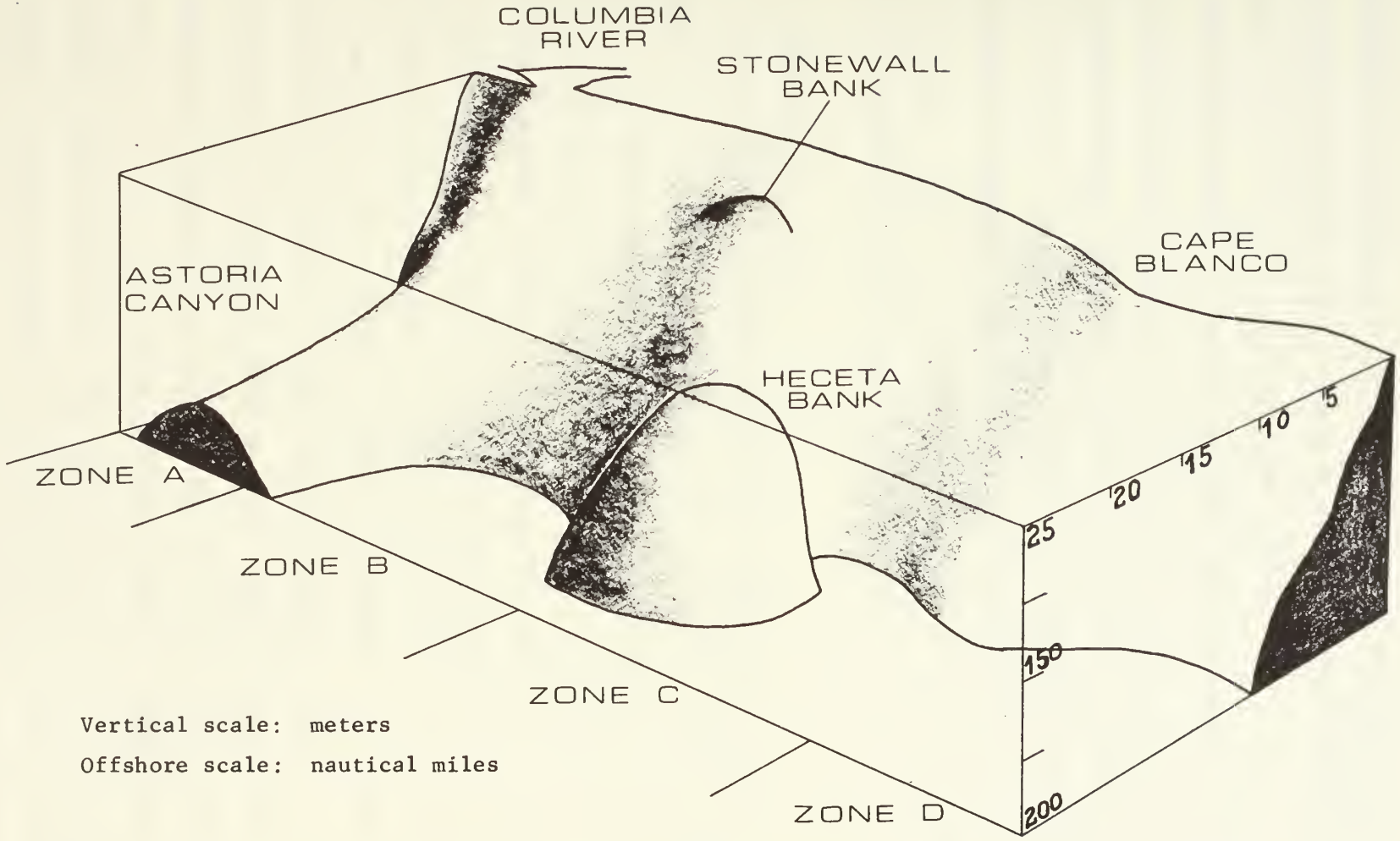

Figure 2. Three-dimensional representation of the approximate topography of the study area.

established by January and disappears by May. It develops inshore of the California Current and may reach 50 miles in breadth and attain speeds of 20 to 40 cm/sec (Schwartzlose, 1963).

The Oregon coast is located approximately in the center of the zone of prevailing westerlies with local winds varying from northwest to southeast throughout most of the year. The barrier presented by the mountains of the Coast Range influences the general wind pattern, deflecting the winds so that they tend to align with the trend of the coast (Cooper, 1958). In regions where the mountains are low, deflection is minimal and normal wind conditions exist.

B. ORGANIZATION OF DATA

The National Oceanographic Data Center (NODC) has on file all hydrographic data taken in this region prior to 1966. Data from 1966 to 1971 are those observations made by the Department of Oceanography of Oregon State University (OSU). The NODC data are filed by 10^{o} Marsden square numbers; number 157 encompasses the area of this study.

Bourke employed a computer program which excluded all data taken more than 25 miles from shore. The data were then grouped by month so that summer and winter seasons could be determined. The summer season included all data sampled in July and August while the winter season included data from December through March. These data were found to be grouped about hydrographic lines frequently sampled by OSU. These lines originate off Astoria (AH line), Tillamook Head (TH line), Depoe Bay (DB line), Newport (NH line), Coos Bay (CH line), and off Brookings (BH line). Along hydrographic lines observations are made at regular intervals at 5, 15, 25, ... nautical miles offshore. Occasionally

additional stations are taken at three and ten miles. As a result, within the study area, most of the data were clustered about hydrographic lines oriented perpendicular to the coast and were further clustered at positions 5, 15, and 25 miles from the coast.

With these points in mind Bourke established a grid system wherein average values of temperature and salinity could be computed for a specified area within the grid network. Average values were computed for depths of 0, 10, 20, 30, 50, 75, 100, 150, and 200 meters.

The study area was divided into four zones as shown in Figure 3. Factors affecting the temperature and salinity were assumed to be uniform or consistent within each zone. The zone boundaries were constructed after having considered the shape of the coastline, location of coastal rivers, bottom topography, and distribution of data. Zone A extends from 46° 16' N to 45° 38' N, Zone B from 45° 38' N to 44° 19' N, Zone C from 44° 19' N to 42°47'N, and Zone D from 42° 47' N to 41° 41' N. Each zone encompasses at least one hydrographic line.

Although the average values apply to a given area, they were assigned to a specific point for calculation purposes. These artificial stations provided a network for the computation of geostrophic velocity and transport within the study area.

C. PREVIOUS STUDIES

Bourke analyzed the data used in this thesis as regards temperature and salinity structure. In general, he found that the surface waters were warmer in summer than in winter. Summer temperatures were 2 to 5°C warmer than winter temperatures with the largest increases occuring off Northern Oregon. Surface temperatures increased with distance offshore

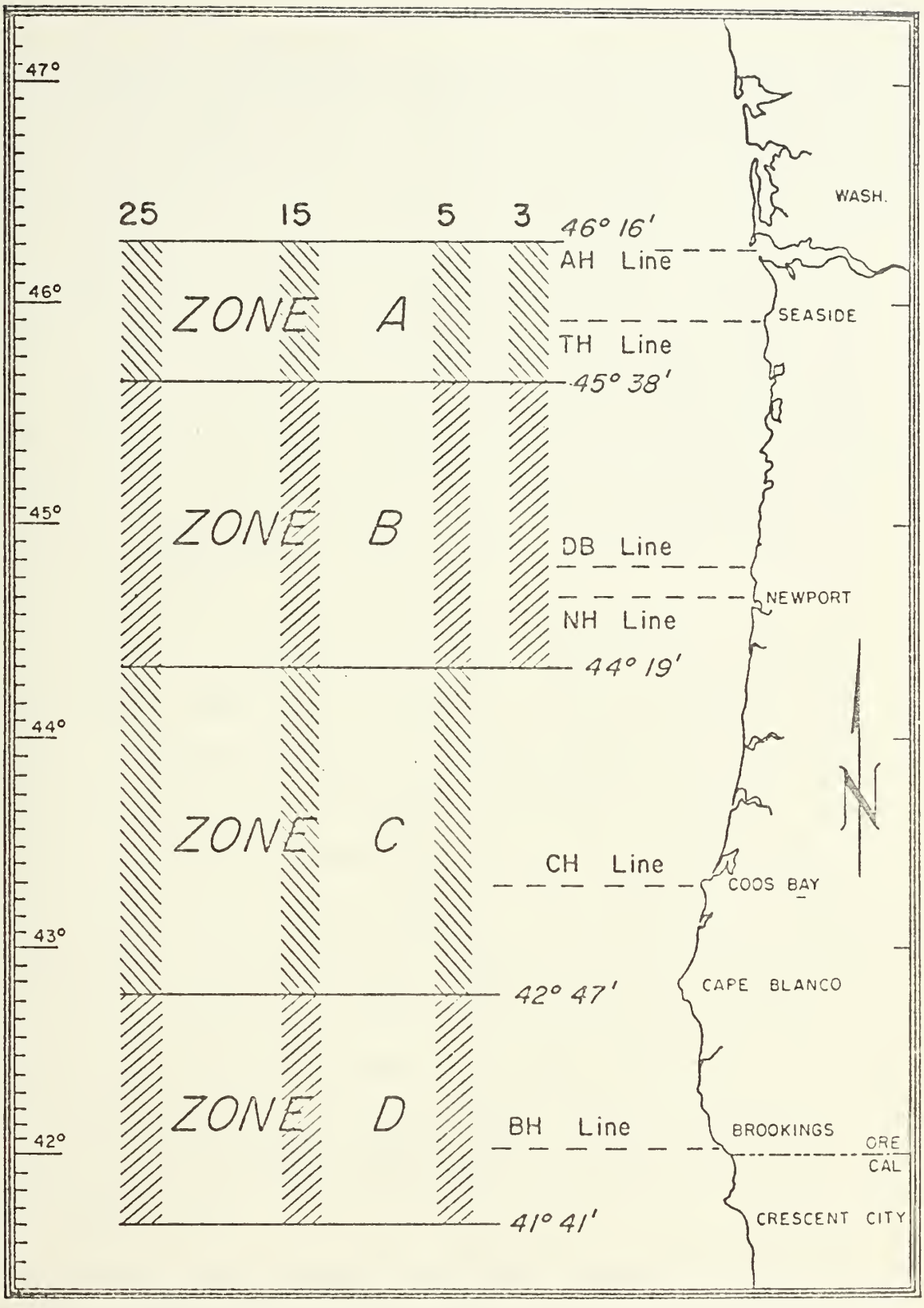

Figure 3. Schematic diagram of data grid showing zone boundaries. Hydrographic lines are shown as dotted lines. (from Bourke, 1971)

in both seasons. The offshore temperature gradient was 4 times larger in summer than winter. In the longshore direction surface temperature increased toward the north in summer while the reverse was true in winter. The temperature gradient was nearly the same in both seasons.

Surface waters were 0.5 to 1.0 ppt more saline in summer than in winter. Surface salinities decreased with distance from shore in summer. In winter surface salinities increased with distance from shore. Salinity gradients in the x (offshore) direction were identical in summer and winter. In both seasons surface salinities increased toward the south. The longshore gradient, however, was twice as large in summer as in winter.

Variability in temperature, salinity, and density with distance from shore was significant in summer but relatively unimportant in winter. A strong thermocline was present in summer from the surface to 30 meters. Winter surface waters were isothermal to 50 meters. A strong halocline was observed in both seasons extending to 75 meters in the summer and 100 meters in winter. In both seasons at 200 meters the temperature and salinity were essentially constant throughout the study area. At 200 meters summer temperatures and salinities were cooler and more saline than winter values due to the strong coastal upwelling occuring during the summer months. Summer values were $6.8 \pm 0.2^{\circ}C$ and 33.98 ± 0.01 ppt; in winter these were $7.7 \pm 0.1^{\circ}C$ and 33.90 ± 0.5 ppt.

The frontal layer (permanent pycnocline), defined by Collins (1964) to be bounded by the 25.5 and 26.0 σ_t surfaces, rises sharply shoreward in summer, but is essentially flat in winter. Its depth in

winter is about 100 meters. During the summer it slopes from a depth of about 50 meters at 25 miles offshore to a depth of about 20 meters at 3 miles offshore. In Zone D it breaks the surface at about 7 miles offshore.

Pavlova (1966) performed a study of the seasonal variations in the California Current and Countercurrent in latitudes 20° to 40°N. Using hydrographic data averaged over 35 years she computed geostrophic velocities and transports relative to 1500 decibars. She also mapped the dynamic topography of the California Current.

In developing a characteristic profile of the California Current and Countercurrent, she chose a cross section oriented perpendicular to the coast around 32° north latitude. A northward countercurrent is observed at depth throughout the year. Except during the spring, a surface countercurrent is also observed throughout the year. Maximum countercurrent velocities (8 to 9 cm/sec) are reached in the summer and autumn at a depth that varies in the course of the year: from 200 to 300 meters at the beginning of the summer and in the autumn, to 100 meters at midsummer. On an annual average, however, the countercurrent at depth is practically a single and uniform flow from 25° N to 35° N and farther.

The strength of the countercurrent is related to the California Current. Maximum velocities for both currents are reached in summer and in autumn when the northerly geostrophic wind is strongest and upwelling is most intense along the coast.

Pavlova also notes that in the upper layers there is an upward and in the lower layers a downward isopycnic slope from the ocean

towards the coast, so that at intermediate depths (100 to 250 meters) a zone of divergence of the isopycnals forms in relation to the position of the profile and the time of year. Her data indicate that the countercurrent reaches maximum development in this zone of divergence, which in August is centered on the 26.0 isopycnic surface.

II. THEORY

A. INTRODUCTION

It is assumed that the long-term mean current is composed of two parts: a baroclinic component arising from the distribution of the internal mass field and a barotropic component arising from the slope of the sea surface. Geostrophy is assumed in order to determine the vertical velocity profile and this is transformed to an absolute profile by the use of data from moored current meters.

B. GEOSTROPHIC VELOCITY

The theoretical development is presented in the left-handed coordinate system where the z axis is positive downward and the y axis is positive northward. The components of velocity, u and v, are directed along the x and y axes, respectively. Pressure is denoted by p, density by ρ, and the eddy viscosity coefficient by A. Other definitions to be used are specific volume, α, defined as the reciprocal of density and the Coriolis parameter, f, defined as $2\Omega\sin\phi$, where ϕ is latitude and Ω is the angular velocity of the earth.

Since north-south (meridional) velocities are being examined, the appropriate equation of motion describes the east-west (zonal) acceleration:

$$\frac{du}{dt} = (2\Omega\sin\phi)v - \frac{1}{\rho}\frac{\partial p}{\partial x} + F_x .$$

The frictional term is chosen to have the form:

$$F_x = \alpha\left[\frac{\partial}{\partial x}(A_H\frac{\partial u}{\partial x}) + \frac{\partial}{\partial y}(A_H\frac{\partial u}{\partial y}) + \frac{\partial}{\partial z}(A_V\frac{\partial u}{\partial z})\right] \quad (1)$$

This equation states that the frictional forces present can be re-

presented as shearing stresses. Furthermore it is assumed that the lateral shearing stresses are minor in comparison with the vertical shearing stresses. The equation of motion can then be written as

$$\frac{du}{dt} = fv - \alpha\frac{\partial p}{\partial x} + \alpha\frac{\partial}{\partial z}(A\frac{\partial u}{\partial z}) \quad (2)$$

where the V notation has been dropped on the vertical eddy viscosity coefficient.

This equation is simplified by two assumptions based on the following considerations:

(a) The data consist of long-term monthly averages of salinity and temperature. These values are further averaged over a seasonal period of two months or more, so that a smoothed seasonal description of the study area may be presented.

(b) Frictional effects, although present, are confined to relatively thin boundary layers (of the order of 20 meters) at the sea surface and along the bottom of the shelf and slope regimes. These effects exert an insignificant influence on the geostrophic interior of the area.

In support of (b) the following calculations are presented for Zone B where sufficient current measurements were available. The average wind speed for July and August is 6.0 m/sec blowing roughly from the north most of these two months (Fleet Numerical Weather Center, Monterey, California). Based on a wind speed of 6.0 m/sec, Neuman's (1966) value for the "effective" eddy viscosity coefficient, A, is 160 gm/cm-sec. The following current measurements were collected by OSU seven nautical miles offshore of Depoe Bay, Oregon, in 100 meters of water, from 23 June to 10 July 1968:

Depth of sensor (m)	u component* (cm/sec)
25	0.9
50	2.1
75	4.8

* Velocities are averages based on common record lengths. (adapted from Pillsbury, et al., 1970)

If A is assumed constant and the above data are used to evaluate $\partial^2 u/\partial z^2$ numerically, one obtains a value of 2.4×10^{-7} $(\text{cm-sec})^{-1}$. The frictional wind stress term is, therefore, of the order of 10^{-5} while the Coriolis term, fv, is of the order of 10^{-3}.

By reason of (a) above, $du/dt = 0$. By reason of (b), $\alpha A \partial^2 u/\partial z^2 \approx 0$, so that the equation for the x component of motion may be expressed as

$$fv = \alpha \frac{\partial p}{\partial x}. \quad (3)$$

It is recognized that the time averaging process which eliminates the time dependence in equation (2) also reinforces the stress terms of equation (1). This result is deemed negligible and equation (3) is used as the governing equation for the distribution of the meridional velocity field.

For small pressure differences, Δp, and small distances, Δz and Δx, one may express the vertical and horizontal pressure gradients as

$$\Delta p = \rho g \, \Delta z$$

$$\text{and} \quad \Delta p = (\partial p/\partial x) \, \Delta x.$$

Eliminating Δp yields

$$g \, \Delta z = (\partial p/\partial x) \, \Delta x.$$

Rewriting the equation leaves

$$g \frac{\Delta z}{\Delta x} = \alpha \frac{\partial p}{\partial x}.$$

In the limit that Δx and Δz approach zero, while the pressure remains constant, one obtains

$$g\left(\frac{\partial z}{\partial x}\right)_p = \alpha \frac{\partial p}{\partial x}. \quad (4)$$

The pressure gradient in equation (3) can now be replaced by the zonal slope of an isobaric surface. The concept of a slope, however, implies the existence of an absolute reference surface (i.e. a level surface), a surface frequently unknown in oceanographic work. Thus the idea of a relative slope is introduced. Given the vertical distances, h_A and h_B, between isobaric surfaces at stations A and B, respectively, the slope of surface p_1 relative to a deeper surface p_2 is given by

$$\left(\frac{\partial z}{\partial x}\right)_p = \frac{h_B - h_A}{L} \quad (5)$$

where L is the distance between stations and station A is east of station B as illustrated in Figure 4.

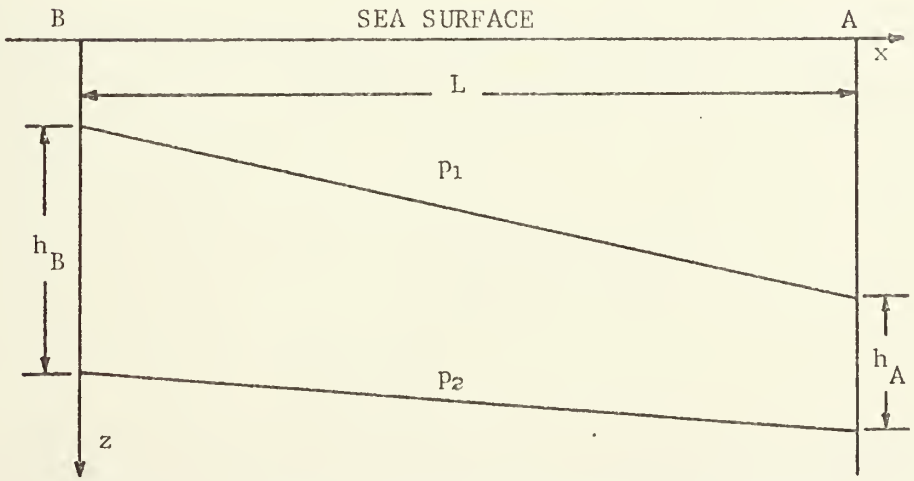

Figure 4. Determination of the slope of the p_1 surface relative to the p_2 surface.

The evaluation of h_A and h_B is accomplished utilizing the concept of geopotential as described by Sverdrup, Fleming and Johnson (1942). The result of their discussion states that a geometrical distance, z, is proportional to the pressure integral of the specific volume of the water column,

$$z = \frac{10}{g} \int \alpha \, dp.$$

A convenient, but arbitrary, choice of units requires that g be specified in m/sec^2, p in decibars (10^5 dynes/cm^2) and α in cm^3/gm. The depth, z, is then specified in meters. Applying this technique to equation (5) yields

$$\left(\frac{\partial z}{\partial x}\right)_p = \frac{10}{gL}\left[\left(\int_{p_1}^{p_2} \alpha \, dp\right)_B - \left(\int_{p_1}^{p_2} \alpha \, dp\right)_A\right]. \quad (6)$$

Substituting equations (3) and (4) into equation (6) gives the relative current perpendicular to the plane between stations A and B,

$$v_1 - v_2 = \frac{10}{fL}\left[\left(\int_{p_1}^{p_2} \alpha \, dp\right)_B - \left(\int_{p_1}^{p_2} \alpha \, dp\right)_A\right]. \quad (7)$$

The integral over pressure is the geopotential distance, D, expressed in dynamic meters. According to Sverdrup, et al., D is defined as the sum of D_o and ΔD, where

$$D_o = D_2 - D_1 = \int_{p_1}^{p_2} \alpha_{\,35,0,p} \, dp$$

$$\text{and } \Delta D = \int_{p_1}^{p_2} \delta \, dp.$$

The standard geopotential distance, D_o, results from integrating over a "standard" water column of salinity equal to 35 ppt and temperature equal to $0^\circ C$. The geopotential anomaly, ΔD, results from integrating

over a water column whose salinity and temperature structure are defined solely in terms of deviations from the structure of the "standard" water column. The symbol, δ, denotes the specific volume anomaly. Rewriting equation (7) gives

$$v_1 - v_2 = \frac{10}{fL}\left[\left(\int_{p_1}^{p_2} \delta\, dp\right)_B - \left(\int_{p_1}^{p_2} \delta\, dp\right)_A\right]. \quad (8)$$

Since the ocean is very nearly in hydrostatic equilibrium and since the decibar was chosen as the dimension of pressure, dp may be replaced by dz, where z is measured in meters. As a working approach, a level sea surface is assumed so that v_1 vanishes. With this assumption, v_2 is necessarily a baroclinic velocity only. It is caused strictly by the distribution of the internal mass field. There is no barotropic component since there is no slope of the sea surface. The integration is performed from the sea surface to the depth of interest, therefore

$$v(z) = v_2 = \frac{10}{fL}\left[\left(\int_{o}^{z} \delta\, dz\right)_A - \left(\int_{o}^{z} \delta\, dz\right)_B\right]. \quad (9)$$

With this formula v(z) is rendered in meters per second. By specifying L in kilometers and omitting the factor of 10 in the numerator, v(z) may be calculated in centimeters per second. An observer, looking at the plane of the stations with station A to the right of station B, will note that a positive current flows away from him while a negative current flows toward him.

By means of a fairly uncomplicated, but lengthy, computer program, the specific volume anomaly may be determined by the appropriate polynomial (Knudsen, 1901). Numerical integration to successive depths

generates the baroclinic velocity profile. However, the profile is still relative to the sea surface which has been assumed level. As it turns out this is usually a poor reference level and the calculated shear must somehow be fixed at a point to provide a more realistic distribution of velocity. Traditionally this has been done by assuming that horizontal motion ceases at some great depth, usually around 1500 decibars (Defant, 1961). The profile is then adjusted to show a zero current at 1500 db. In shallower areas a more positive approach is to measure the current at some depth (or depths) and then adjust the baroclinic profile to make the best fit to the data. In effect, this amounts to adding a barotropic component to the velocity profile. This latter technique is equivalent to a physical determination of the reference level. Both techniques allow the computation of the sea surface slope once the shear has been altered. In the computer program, the user specifies a reference level, and the vertical velocity profile is adjusted so that the current is zero at this depth. Knowledge of the correct reference level is imperative if the profiles are to provide useful information.

C. VOLUME TRANSPORT

When describing oceanic circulation, a quantity of interest is the volume transport between two stations. Consider a plane section bounded on either side by stations A and B, at the top by the sea surface and at the bottom by some isobath, d. The volume transport is a measure of the amount of water passing through this plane section per unit time. Given the velocity as a function of depth, the volume transport is

$$T = L \int_{o}^{d} v \, dz. \quad (10)$$

Using the computer program mentioned previously, it is a simple matter to insert the adjusted velocity values into this equation and perform the indicated integration. Equation (10) is preferred to the often quoted equation,

$$T = \frac{10}{f} \int_{o}^{d} (\Delta D_B - \Delta D_A) \, dz. \quad (11)$$

This equation is developed by making the following substitution for v in equation (10):

$$v = \frac{-10}{f} \frac{\partial(\Delta D)}{\partial x} \approx \frac{10}{f} \frac{\Delta D_B - \Delta D_A}{L}$$

where D_A and D_B are the geopotential anomalies at stations A and B, respectively, in the configuration described earlier. Application of equation (11) requires that the velocity must vanish at some depth. No such requirement is imposed on equation (10). Using the adjusted profile, transport in water layers can be calculated and then summed to give total volume transport. To a sufficient degree of accuracy, the mass transport may be determined by multiplying the volume transport by an average density value.

D. THERMAL WIND RELATIONSHIP

The thermal wind equation, sometimes written as

$$\frac{\partial v}{\partial z} = \frac{-g}{f} E \, s \quad (12)$$

will be referred to in the discussion of procedure. The simplifying conditions needed for the development of this expression are given by Pillsbury (1972) in a very straight-forward derivation. Using the

same coordinate system as before and with only the pressure and Coriolis forces acting in the east-west direction, the equation of motion becomes

$$\rho \, fv = \frac{\partial p}{\partial x} .$$

Using the hydrostatic equation,

$$\rho \, g = \frac{\partial p}{\partial z}$$

the pressure term is eliminated by cross differentiation to leave

$$\frac{\partial v}{\partial z} = \frac{g}{f\rho} \frac{\partial \rho}{\partial x} - \frac{v}{\rho} \frac{\partial \rho}{\partial z} . \quad (13)$$

In the study area, v is of the order of 10 cm/sec making

$$\frac{g}{f\rho} / \frac{v}{\rho} \approx 10^{-5} .$$

The slope of the isopycnal,

$$s = \left(\frac{\partial z}{\partial x}\right)_\rho = - \frac{\partial \rho / \partial x}{\partial \rho / \partial z}$$

is not often less than 10^{-3} in the study area (Pillsbury, 1972). Therefore the ratio,

$$\frac{g}{f\rho} \frac{\partial \rho}{\partial x} / \frac{v}{\rho} \frac{\partial \rho}{\partial z}$$

is of the order of 10^{3}. Thus the second term on the right-hand side of (13) may be neglected, and the vertical shear may be written as

$$\frac{\partial v}{\partial z} = \frac{g}{f\rho} \frac{\partial \rho}{\partial x} . \quad (14)$$

Now the static stability is given by

$$E = \frac{1}{\rho} \frac{\partial \rho}{\partial z}$$

and the product of the isopycnal slope and the static stability is

given by

$$E_s = -\frac{1}{\rho}\frac{\partial \rho}{\partial x} .$$

Substituting this expression in (14) leaves equation (12),

$$\frac{\partial v}{\partial z} = \frac{-g}{f} E_s .$$

III. PROCEDURE

A. INTRODUCTION

The original objective of this study was to compute relative seasonal velocity profiles in the four zones and then adjust these profiles to agree with observed current measurements. It was thought that this procedure would develop a reliable long-term mean picture of the water circulation over the Oregon and Northern California shelf-slope area. With the corrected velocity profiles, meaningful longshore transport computations could be made.

These plans had to be modified due to the lack of sufficient current observations. The best measurements available were collected by Oregon State University's Department of Oceanography. These were taken in coastal waters off Depoe Bay and Newport, Oregon, in 1966, 1967, 1968, and 1969. They were used to adjust the velocity profiles of Zone B. Other measurements were taken by the University of Washington's Department of Oceanography. It was hoped that the latter could be used in the profiles of Zone A since they were collected near the mouth of the Columbia River. This was not the case, however, since the measurements that were collected during the appropriate months, were collected at depths deeper than the available hydrographic data. No current data were located for Zones C and D. In addition scarcity of winter hydrographic data in Zone D precluded the formation of statistically significant average values for that season.

Consequently the results presented are not absolute, but do illustrate a fairly accurate description of the variations in relative water movements from summer to winter and alongshore from north to south.

B. METHOD

A computer program was obtained to compute the geostrophic velocities via equation (9) as developed in section II. The use of geostrophy is based on the assumption that the frictional boundary layers at the bottom and at the sea surface are small in comparison with the depth of most of the area. The wind, which is an important consideration in this region, is assumed to control only the barotropic component of the flow due to its influence on the sea surface slope.

The problem of wind stress has been reasonably refuted by the numerical example cited in the theoretical development, but some assumptions were involved there that need to be examined. The 1968 current data used in the determination of $\partial^2 u/\partial z^2$ were collected in a period that did not fall entirely within the months of July and August, the period used for geostrophic calculations. It was assumed that during these months the currents did not vary significantly from the observed currents during the time 23 June to 10 July 1968. Also specific wind statistics were not available for the station at the time the current measurements were being recorded. Consequently, the wind speed at the time of observation was assumed to be the long-term mean wind speed as tabulated by FNWC for the months of July and August (July mean, 12.6 kt.; August mean, 11.0 kt.).

The wind speed was the determining factor in choosing a value for the eddy coefficient, A. In order to increase the magnitude of the frictional term to the point where it would be significant with respect to the Coriolis term, it is estimated that the mean wind speed from 23 June to 10 July 1968 would have to have been about 20 knots.

The applicable eddy coefficient would then have a value of about 580 gm/cm-sec instead of the value 160 gm/cm-sec. The frictional term would therefore amount to about 10 percent of the Coriolis term and probably could not be neglected in treating the equation of motion.

The assumption that mean wind conditions prevailed at the time of data collection might be open to question. Nevertheless, one wishes to have confidence in long-term mean data when applying it to any one particular time segment. If the number of observations of wind speed is large and these observations are concentrated about the mean, then the assumption of mean conditions is probably adequate. This is the case in the study area during the summer.

The irregular topography of the area will complicate the geostrophic flow pattern but will not affect the condition of geostrophy *per se* except in the very shallow regimes. Dynamically the topographic anomalies do not appear to influence the hydrographic data. For a given depth, temperature and salinity do not vary significantly in the longshore direction within the zone boundaries. This fact is one of the points considered by Bourke when he first established the grid system of this area.

IV. RESULTS

A. VELOCITY FIELDS IN SUMMER

The most pronounced results are presented in Figures 5 through 8. These profiles represent geostrophic meridional velocities that were computed relative to the deepest common data point between stations. They do not represent accurate absolute values, but they are reliable in terms of the distribution of vertical shear. Examined in this light, the profiles illustrate some interesting patterns.

The diagram for Zone A during the summer shows a surface jet starting at 13 to 15 nautical miles offshore and extending to the seaward limit of the data (25 n. mi.). This jet is the result of the discharge from the Columbia River. Using theory developed for surface discharges from ocean outfalls, Bourke has shown that the temperature-salinity characteristics of the core of the Columbia River plume remain intact to a distance of 10 to 15 miles from the mouth of the river. The jet in Zone A profile, therefore, represents a southward flowing mass of warm and relatively fresh water that has been discharged from the jetties at the mouth of the Columbia. The averaged hydrographic data support this analysis since cold saline oceanic water is found on both sides of the jet which is characterized by its warm, relatively fresh flow.

The Columbia River discharge exerts a minimal influence on Zones B and C. In these zones the distinctive temperature-salinity of the core of the Columbia River plume is not present and oceanic water predominates. The Zone B diagram also shows a surface jet located in the interior of the zone. Other barotropic data could shift the location

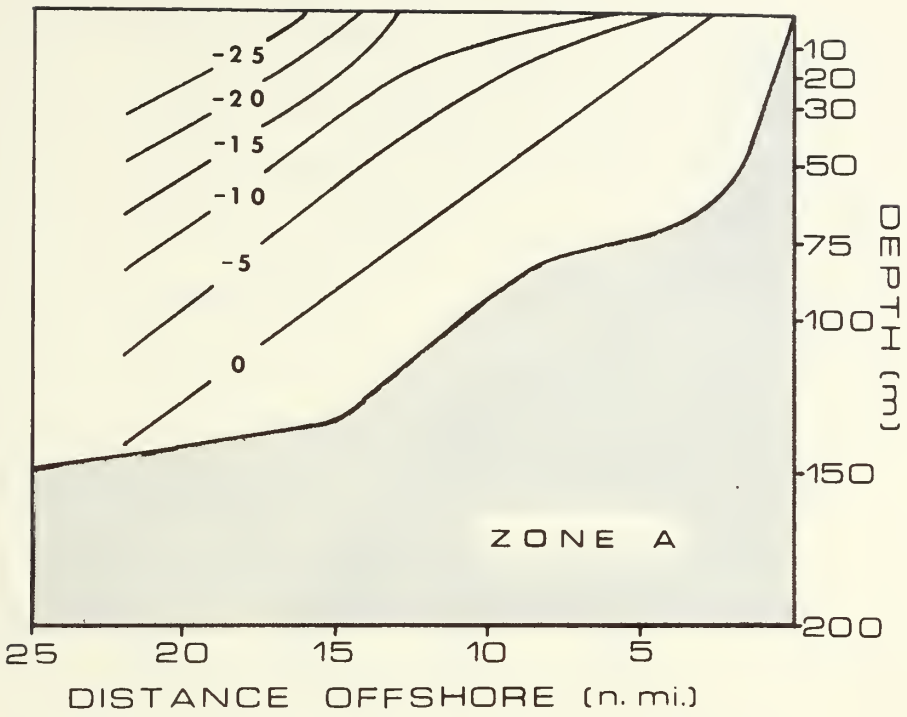

Figure 5. Average summer meridional velocity field for Zone A in cm/sec.

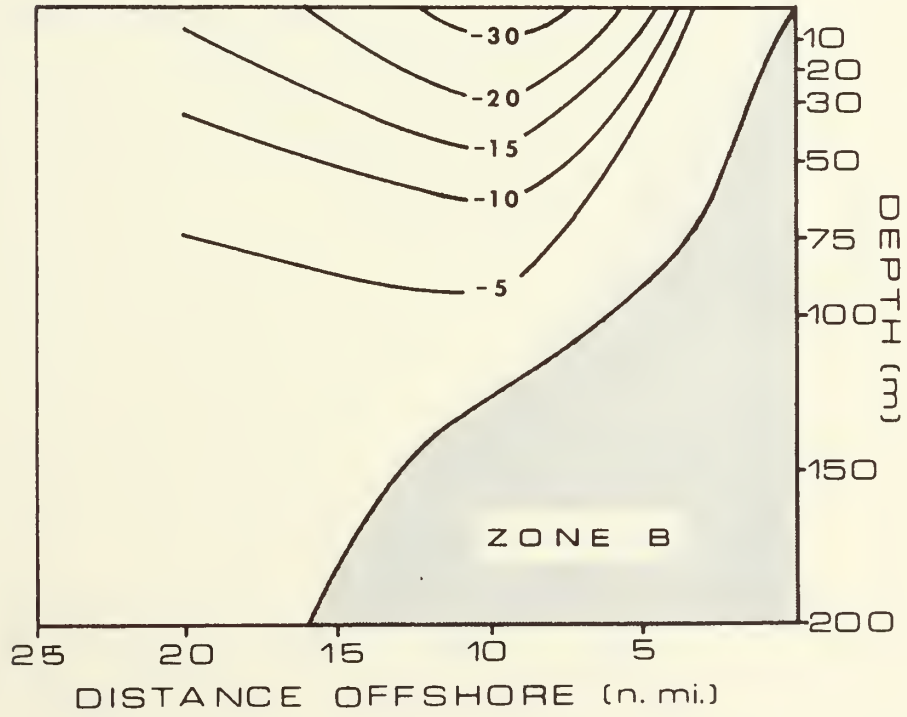

Figure 6. Average summer meridional velocity field for Zone B in cm/sec.

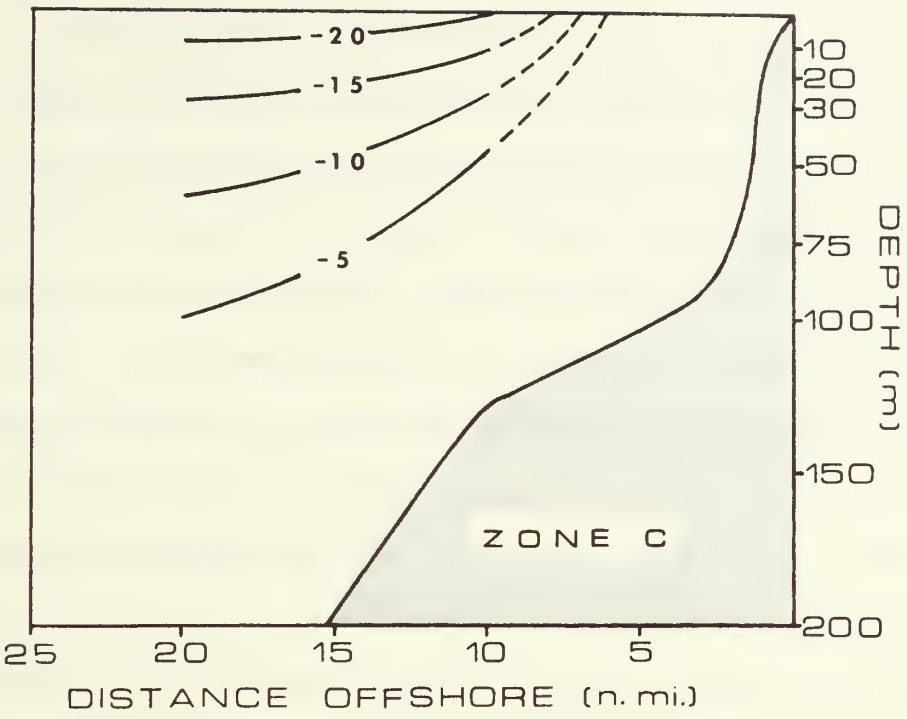

Figure 7. Average summer meridional velocity field for Zone C in cm/sec.

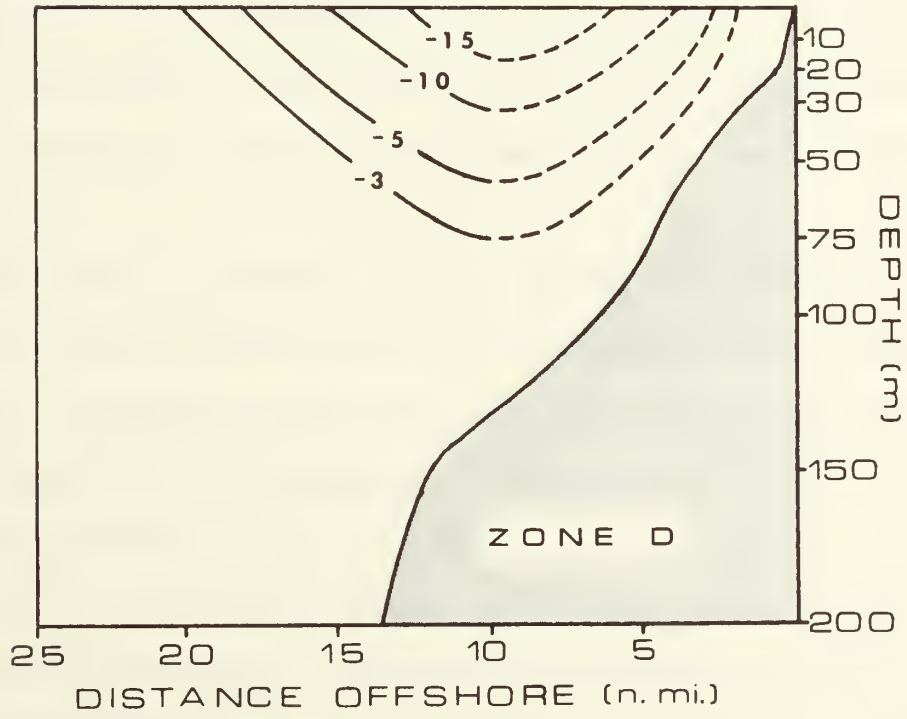

Figure 8. Average summer meridional velocity field for Zone D in cm/sec.

of the jet east or west, but 10 nautical miles is a reasonable position. This jet flow is a characteristic predicted by a numerical model of this area developed by O'Brien and Hurlburt (1972). They used a model consisting of two homogenous layers coupled together by shearing stresses but not by mixing. The system is driven by a meridional wind stress. Their results predict a southerly current centered 10 kilometers offshore, in reasonable agreement with the value of 10 nautical miles (20 km.) predicted here.

The Zone C profile is based on less data than Zones A and B. Of primary concern here is the absence of sufficient hydrographic data to construct long-term mean values at a position less than 5 miles off the coast. As a result any isotachs drawn shoreward of 10 miles are speculation. Nevertheless, the profile indicates that the jet, if it is the same one from Zone B, has moved seaward. It is noteworthy that here, as in the other zones, the jet remains positioned above the steeper portion of the permanent pycnocline as described by Bourke.

What might be happening in Zone C is that the northerly wind along the coast is being constricted and accelerated as it passes Cape Blanco. The physical result is an area of uniformly high winds and decreased pressure. Consequently one observes more intense upwelling in this area than in Zone B.

Zone D, located just south of Cape Blanco, appears to exhibit the effect dramatically. Upwelling has intensified as shown by the presence of cold saline water farther out to sea and by the permanent pycnocline breaking the surface at about 7 miles offshore as mentioned

earlier.

As discussed beforehand these profiles were computed relative to the deepest common data point between stations. One cannot expect this method to be very accurate in an absolute sense, but it is more realistic than assuming surface currents are zero. As a check on the procedure thus far, Figures 9 and 10 are presented. These are profiles for Zone B that have been corrected using current measurements from moored current meters. The data, collected and processed by OSU, are listed in Tables I and II.

The measurements from 1966 indicate a vertical shear of 4.7×10^{-3} sec^{-1} between the depths of 20 and 60 meters at 5 nautical miles offshore. Using mean hydrographic values in the thermal wind relation yields a vertical shear of about 4.2×10^{-3} sec^{-1} between stations B-05 and B-15 over an interval of depth centered at 40 meters. The 1969 observations show a vertical shear of 2.6×10^{-3} sec^{-1} between the depths of 20 and 80 meters at 15 nautical miles offshore. Between stations B-15 and B-25, the average hydrographic data in the thermal wind relation gives a vertical shear of 1.6×10^{-3} sec^{-1} over an interval of depth centered at 50 meters. The agreement between the measured shear and the predicted geostrophic shear is reassuring and lends a little more credence to the adjusted profiles.

Consistent with the profiles discussed previously, the adjusted profiles (Figures 9 and 10) confirm the existence of the surface jet. The presence of a subsurface countercurrent is indicated by the 1966 profile. These results have also been noted by Mooers, Collins, and Smith (1972). Their data included that of Table I and a line of

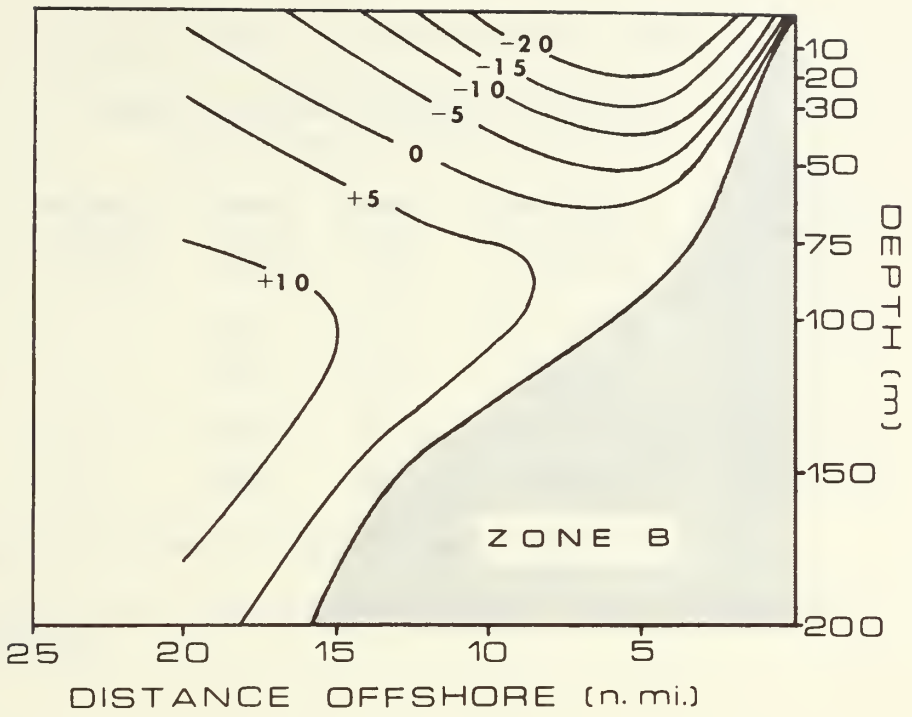

Figure 9. Summer meridional velocity field for Zone B adjusted with 1966 current observations.

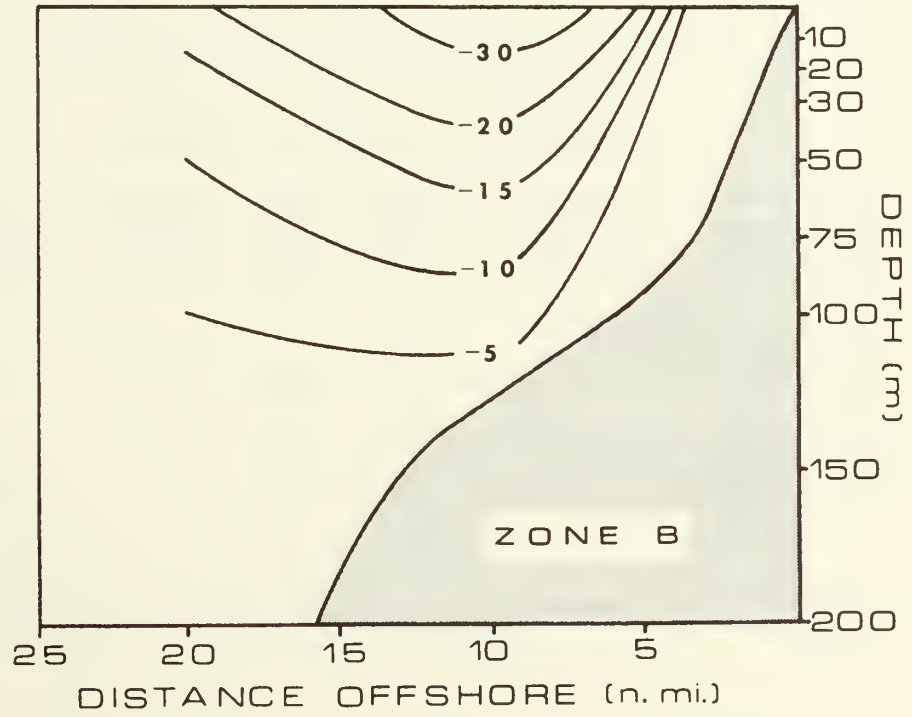

Figure 10. Summer meridional velocity field for Zone B adjusted with 1969 current observations.

Table I.* Mean Current Statistics, 1966

(based on hourly averages for common record length of 339 hours)

Depoe Bay Station	Distance offshore (n mi)	Water depth (m)	Sensor depth (m)	Eastward component** (cm/sec)	Northward component** (cm/sec)
5	5	80	20	-2.2 ± 11	-17.9 ± 12
5	5	80	60	2.8 ± 6	0.7 ± 9
10	10	140	20	4.5 ± 10	-12.1 ± 9
15	15	200	60	6.0 ± 6	7.9 ± 13

* Adapted from Mooers, Collins, and Smith (1972).

** Velocities are presented as the mean value ± the standard deviation.

Table II.* Mean Current Statistics, 1969

(based on total record lengths acquired in August and September)

Station (Newport or Depoe Bay)	Distance offshore (n mi)	Water depth (m)	Sensor depth (m)	Eastward component** (cm/sec)	Northward component** (cm/sec)
NH-3	3	50	20	0.7 ± 7	-4.4 ± 16
DB-7	7	100	40	-6.1 ± 11	-21.1 ± 19
NH-15	15	100	20	-9.9 ± 16	-18.1 ± 16
NH-15	15	100	80	-3.5 ± 14	-2.8 ± 12

* Adapted from Huyer, et al. (1971).

** Velocities are presented as the mean value ± the standard deviation.

hydrographic stations taken in late July, 1966, off Newport, Oregon. The velocity field presented by Mooers, et al. differs only slightly from the profile presented here based on long-term mean hydrographic data and the data from Table I. The 1966 profile centers the southward flowing jet at about 5 nautical miles (10 km.), in better agreement with the results of O'Brien and Hurlburt. The northward undercurrent apparently does not break the surface as suggested in Figure 9. Mooers, et al. indicate that in 1966 the surface flow was all southerly at least as far as 60 miles offshore. They report that the undercurrent may have come within about 10 meters of the surface that summer.

B. VELOCITY FIELDS IN WINTER

The winter profiles are presented in Figures 11 through 13. Prior to assuming a reference level at depth, the relative (baroclinic) current values were observed to be very small, illustrating the importance of the barotropic component during winter. A zonal sea surface slope of one millimeter per kilometer, corresponding to a current speed of the order of 10 cm/sec, would be sufficient to reverse the flow at any point in any of the zones.

In spite of such small geostrophic velocities a description of a characteristic flow pattern is attempted. It is felt that the long-term nature of the data used in this analysis provides a firmer ground for such an attempt.

Nearshore surface waters in Zones A and B are responding to the wind stress while the offshore and deeper waters are moving under the influence of the large scale oceanic circulation. Current velocities

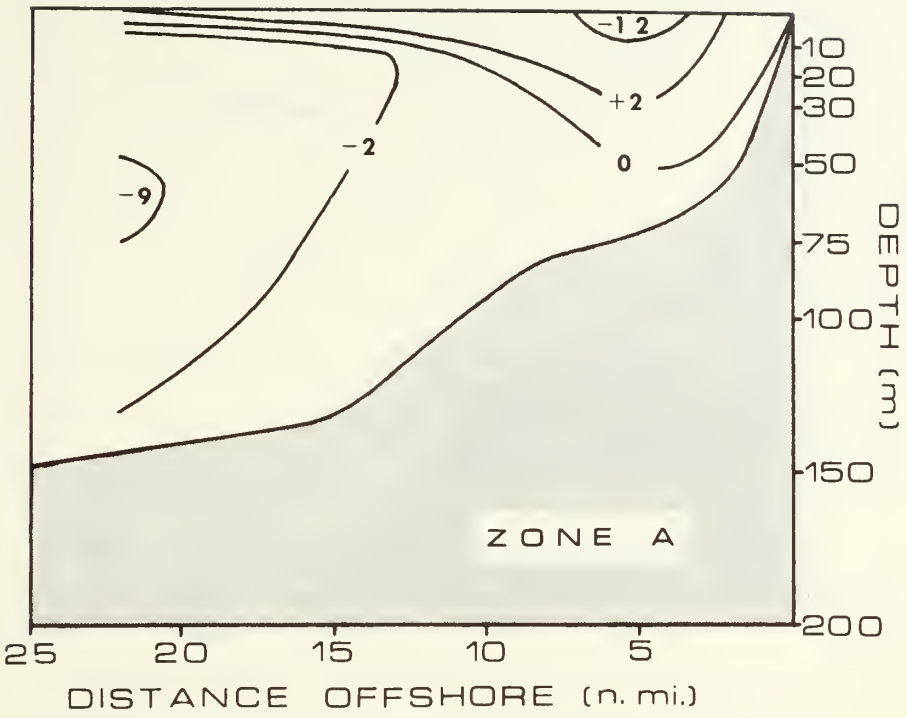

Figure 11. Average winter meridional velocity field for Zone A in cm/sec.

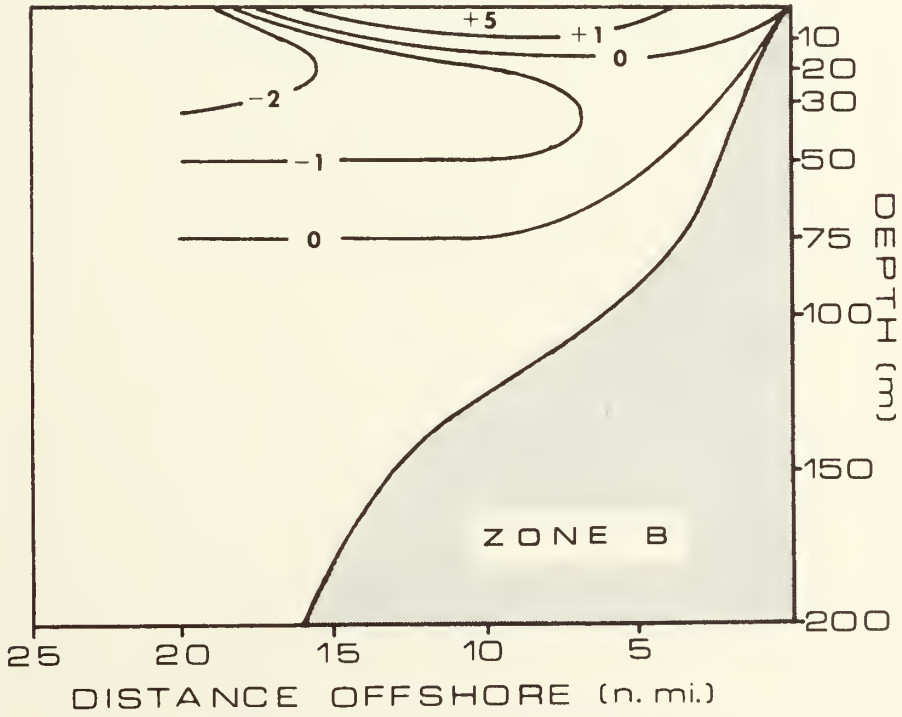

Figure 12. Average winter meridional velocity field for Zone B in cm/sec.

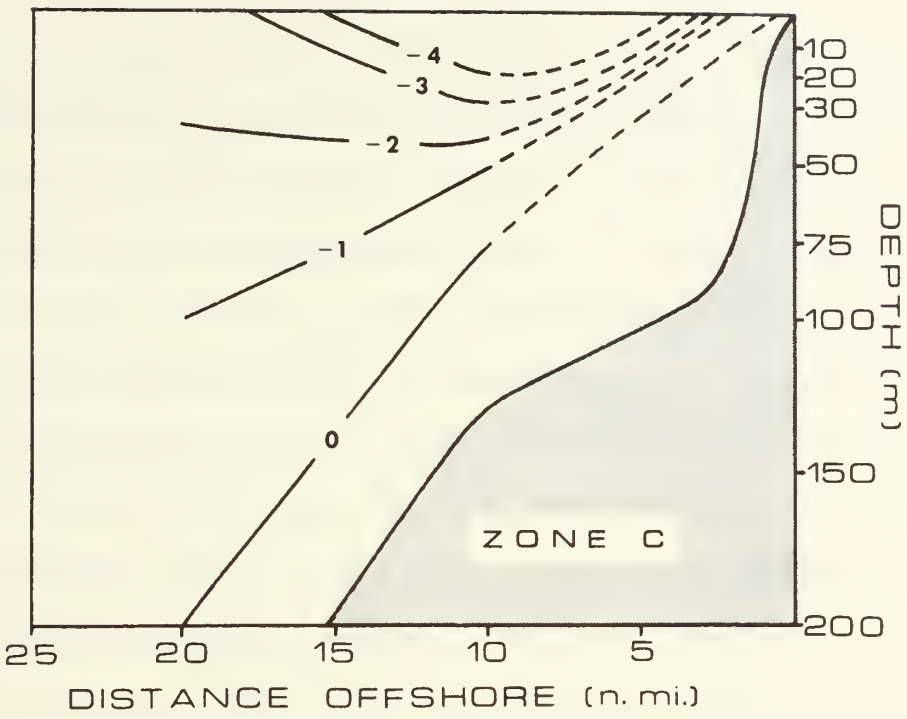

Figure 13. Average winter meridional velocity field for Zone C in cm/sec.

are greatly reduced from the summer values due to the nearly level isopycnal surfaces. Runoff and water piled up onshore by the wind contribute a northerly barotropic component to the circulation.

The University of Washington has made a few current observations during the winter season at moorings near the Astoria Canyon (Hopkins, 1971). Unfortunately, these observations were not sufficiently distributed spatially to allow an absolute rendition of the velocity field. In each of these cases, however, the mean northerly component was only slightly larger (in the sense of being more positive) than the predicted geostrophic component. This fact illustrates two points: that the fresh water runoff and the water piled up onshore by the prevailing wind govern the barotropic component of the velocity and that this barotropic component is not very large.

C. VOLUME TRANSPORT

Volume transports were computed using equation (10). As in the velocity computations, the deepest depth of the data common to the two stations was used as the reference level. Again it is cautioned that this is not necessarily the correct level of no horizontal motion, but it is better than a level sea surface approximation.

The results of this endeavor are presented in Tables III and IV. As expected, the transports are uniformly small, the winter transports being roughly an order of magnitude smaller than the summer transports. (This observation is probably correct; however, it is not completely justified from an inspection of the tables alone. The winter data are generally shallower than the summer data, thereby eroding a basis for comparison.) Reflecting the structure of the velocity fields, the trans-

Table III. Geostrophic Meridional Transports (Summer)

Stations	Volume Transport (Sverdrup)	Direction	Reference Level (m)
A-03/A-05	0.010	S	50
A-05/A-15	0.067	S	75
A-15/A-25	0.411	S	200
B-03/B-05	0.018	S	75
B-05/B-15	0.201	S	150
B-15/B-25	0.193	S	200
C-05/C-15	0.119	S	75
C-15/C-25	0.287	S	200
D-05/D-15	0.134	S	100
D-15/D-25	0.065	S	200

Table IV. Geostrophic Meridional Transports (Winter)

Stations	Volume Transport (Sverdrup)	Direction	Reference Level (m)
A-03/A-05	0.001	N	50
A-05/A-15	0.006	S	75
A-15/A-25	0.198	S	200
B-03/B-05	0.001	N	50
B-05/B-15	0.002	S	75
B-15/B-25	0.023	S	75
C-05/C-15	0.034	S	75
C-15/C-25	0.043	S	200

port appears to be southward in both summer and winter. While this result is probably true for the summer months, it is uncertain that this is the case during the winter months. Deeper data and an accurate determination of a reference level could drastically change the winter transports. The small nearshore northward transport observed in Zones A and B during the winter shows the effect of the wind in moving the surface waters.

V. CONCLUSIONS

The fact that long-term data were used in this discussion allows more general statements to be made than could be made otherwise. The surface jet, for example, is shown to be a regular phenomenon of the summer season. Its position above the steepest portion of the upturned pycnocline and its absence in winter tie it to the occurrence of coastal upwelling. The fact that it is a dominant feature of the average summer velocity fields indicates that it must be a steady state event or at least an average of a series of consistent events. Furthermore, the jet is shown to be a characteristic of most of the Oregon and Northern California coastline.

Mooers, et al. have shown that a two-layered baroclinic model of the flow over the Oregon shelf and slope is at least partially valid. They postulate that the barotropic and baroclinic radii of deformation should provide fundamental length scales. The barotropic radius of deformation is defined as the distance a shallow water wave would travel in an inertial period: $R_{barotropic} = (gH)^{\frac{1}{2}} f^{-1}$. The baroclinic radius of deformation is defined as the distance an internal wave would travel along the interface between a shallow upper layer and a deep lower layer of water in the same inertial period: $R_{baroclinic} = (gD\ \Delta\rho/\rho)^{\frac{1}{2}} f^{-1}$. The estimated values are $R_{barotropic}$ = 2000 kilometers and $R_{baroclinic}$ = 20 kilometers. By plotting the depth of the pycnocline as a function of offshore distance on semi-logarithmic axes, Mooers, et al. confirmed the exponential character of the "interface" and determined its radius of deformation to be about 40 kilometers over the shelf and 70 kilometers

over the slope. By comparison then, the water is deemed sufficiently stratified to warrant use of a two-layered (baroclinic) model, although different length scales are in effect over the shelf and the slope regimes.

Without becoming involved in cause and effect arguments, it is asserted that the longshore northerly wind, acting on a relatively thin surface layer, moves water offshore. This lighter surface water moves seaward without significantly disturbing the lower heavier water and causes a pressure gradient force directed onshore, which in turn gives rise to a southward flow. Because the southerly flow diminishes seaward, vorticity is decreased (f = constant, $\partial v/\partial x < 0$). If potential vorticity is to be conserved (Stommel, 1966), then the thickness of the surface layer must decrease in the vicinity of the horizontal shear. Thus one observes the surface jet, the sloping pycnocline, and upwelling as interrelated phenomena.

Another feature that appears to be related to the upwelling process is the poleward flowing undercurrent. The presence of this subsurface flow has been reported by Mooers, et al. and by other workers, but no theory has been developed to explain it. It is undeniably present in the 1966 profile of Zone B (Figure 9) and, given more shallow reference levels for geostrophic computations, it is not difficult to imagine its presence at the seaward edge of the profiles presented in Figures 5 through 8.

It is reasonable to expect that the inclined isopycnals nearshore are capable of producing an offshore pressure gradient force if the sea surface does not develop enough slope to counteract it. Under

the proper conditions therefore, one may observe the resulting northward baroclinic flow located beneath the pycnocline and offshore. In the shallow shelf regime, the effect is masked by shearing stresses with the bottom and with the nearshore surface jet. This may explain why the subsurface flow is found during some summers and not found during others.

These conclusions are compatible with those of Mooers, et al. They are in basic agreement with the results of O'Brien and Hurlburt, but here there is a notable discrepancy. Upwelling is known to consist of a transient and a steady state condition. This discussion cannot provide an insight into any transient solutions, but it does indicate that the nearshore jet and possibly the subsurface flow develop into steady state features. O'Brien and Hurlburt, in obtaining the nearshore jet, do not permit this result. Indeed their model does not have a steady state solution so that a discussion of such fundamental differences may not be valid.

VI. SUMMARY

The features observed in the study area are attributable to general oceanic circulation and to local wind and climate. The California Current is the main influence on water movement over the shelf and slope. In general, the flow is southward regardless of the season. Summer winds are northwesterly while winter winds are southeasterly. These winds govern the sea surface slope and thereby determine the barotropic flow during the different seasons. Surface waters respond to the wind field and, in general, flow parallel to it. Climate along the Oregon coast provides plentiful fresh water runoff during the winter and considerably less runoff during the summer. The influence of the Columbia River discharge that is felt so strongly in Zone A during the summer is much less evident during the winter due mainly to the shift in wind.

As a result of these characteristics more activity is observed in the summer than in the winter. The summer wind pattern stimulates the process of upwelling which causes tilting of the isopycnals which in turn generates the baroclinic flow. The winter wind pattern piles up water onshore but apparently to no great extent. Consequently there is little barotropic flow and even less baroclinic flow.

Summer circulation is characterized by the upwelling of cold saline water next to the coastline. Typically the surface salinity increases and the surface temperature decreases shoreward and southward indicating more intense upwelling in the lower latitudes of the area. Also observed during the summer is a nearshore surface jet flowing southward. The surface jet occurs in the region above the

steepest portion of the permanent pycnocline where the near surface isopycnals have relatively small slope. In Zone A the jet appears to be caused by the discharge of the Columbia River, whereas in the other three zones it appears to be intimately related to the upwelling process. A subsurface poleward flow is observed but is not conclusively documented as a regular occurrence. This flow develops below the pycnocline in a region where the isopycnals are tilted sharply under the influence of upwelling.

Winter flow is characterized by small barotropic and baroclinic components. Surface salinities and temperatures increase seaward and southward indicating the greater effect of runoff in the higher latitudes of the study area. The very small velocities presented in Figures 11 through 13 suggest that no distinctive longshore flow pattern exists during the winter season, although the surface waters in Zones A and B appear to be responding to the wind field.

In both summer and winter the volume transport is mostly southward. Winter transports are consistently less than summer transports and they are usually less by an order of magnitude.

VII. BIBLIOGRAPHY

Bourke, R.H. 1971. A study of the seasonal variation in temperature and salinity along the Oregon-Northern California coast. Ph.D. thesis. Oregon State Univ., Corvallis. 107 numb. leaves.

Collins, C.A. 1964. Structure and kinematics of the permanent oceanic front off the Oregon coast. Master's thesis. Oregon State Univ., Corvallis. 53 numb. leaves.

Cooper, W.S. 1958. Coastal sand dunes of Oregon and Washington. Geological Soc. of Amer., Memoir 72. 169 p.

Defant, A. 1961. Physical Oceanography, Vol. I. Macmillan, New York, N.Y. 729 p.

Dodimead, A.H., F. Favorite and T. Hirano. 1963. Review of oceanography of the Subarctic Pacific region. Int. N. Pac. Fish. Comm., Bull. 13, pt. II. 195 p.

Hopkins, T.S. 1971. Velocity, temperature and pressure observations from moored meters on the shelf near the Columbia River Mouth, 1967 - 1969. Dept. of Oceanography, Univ. of Washington, Seattle. (Special Rpt. 45, Ref. M71-27) 143 p.

Huyer, A., J. Bottero, J.G. Pattullo and R.L. Smith. 1971. A compilation of observations from moored current meters and thermographs, Vol. V. Oregon continental shelf. 31 July - 21 September, 1969. Dept. of Oceanography, Oregon State Univ., Corvallis. (Data Rpt. 46, Ref. 71-1) 39 p.

Knudsen, M. 1901. Hydrographic Tables. G.E.C. Gad, Copenhagen, Tutein and Koch, Copenhagen, 1959.

Mooers, C.N.K., C.A. Collins and R.L. Smith. 1972. The dynamic structure of the frontal zone in the coastal upwelling region off Oregon. J. of Phys. Oceanography. (in press)

Neumann, G. and W.J. Pierson, Jr. 1966. Principles of Physical Oceanography. Prentice-Hall, Englewood Cliffs, N.J. 545 p.

O'Brien, J.J. and H.E. Hurlburt. 1972. A numerical model of coastal upwelling. J. of Phys. Oceanography. 2(1): 14-26.

Pavlova, Yu.V. 1966. Seasonal variations of the California Current. Oceanology. 6(6): 806-814 (Trans.)

Pillsbury, R.D., R.L. Smith and J.G. Pattullo. 1970. A compilation of observations from moored current meters and thermographs, Vol. III. Oregon continental shelf. May-June, 1967; April-September, 1968. Dept. of Oceanography, Oregon State Univ., Corvallis. (Data Rpt. 40, Ref. 70-3) 102 p.

Pillsbury, R.D. 1972. A description of hydrography, winds and currents during the upwelling season near Newport, Oregon. Ph.D thesis. Oregon State Univ., Corvallis. 163 numb. leaves.

Schwartzlose, R.A. 1963. Nearshore currents of the western United States and Baja California, as measured by drift bottles. Calif. Coop. Oceanic Fish. Invest. Rpts. Vol. IX: 15-22.

Stommel, H. 1966. The Gulf Stream. University of California Press, Berkeley, Calif. 248 p.

Sverdrup, H.U., M.W. Johnson and R.W. Fleming. 1942. The Oceans: Their Physics, Chemistry, and General Biology. Prentice-Hall, Englewood Cliffs, N.J. 1087 p.

INITIAL DISTRIBUTION LIST

		No. Copies
1.	Defense Documentation Center Cameron Station Alexandria, Virginia 22314	2
2.	Library, Code 0212 Naval Postgraduate School Monterey, California 93940	2
3.	Oceanographer of the Navy The Madison Building 732 North Washington Street Alexandria, Virginia 22314	1
4.	Dr. N.A. Ostenso Code 480D Office of Naval Research Arlington, Virginia 22217	1
5.	Department of Oceanography Naval Postgraduate School Monterey, California 93940	3
6.	Asst. Professor R.H. Bourke, Code 58Bf Thesis Advisor Department of Oceanography Naval Postgraduate School Monterey, California 93940	1
7.	Asst. Professor J.A. Galt, Code 58Gl Department of Oceanography Naval Postgraduate School Monterey, California 93940	1
8.	LT B.L. Koblitz, Code 58Kj Department of Oceanography Naval Postgraduate School Monterey, California 93940	1
9.	Dr. C.N.K. Mooers School of Marine and Atmospheric Science University of Miami 10 Rickenbacker Causeway Miami, Florida 33149	1

10.	Dr. R.L. Smith Department of Oceanography Oregon State University Corvallis, Oregon 97331	1
11.	Dr. J.J. O'Brien Department of Oceanography Florida State University Tallahassee, Florida 32306	1
12.	Dr. Y. Hsueh Department of Oceanography Florida State University Tallahassee, Florida 32306	1
13.	ENS W.F. Whitson, USN 1042 Halsey Drive Monterey, California 93940	3
14.	Asst. Professor E.B. Thornton, Code 58Tm Department of Oceanography Naval Postgraduate School Monterey, California 93940	1

Security Classification

DOCUMENT CONTROL DATA - R & D

(Security classification of title, body of abstract and indexing annotation must be entered when the overall report is classified)

1. ORIGINATING ACTIVITY (Corporate author)

Naval Postgraduate School
Monterey, California

2a. REPORT SECURITY CLASSIFICATION

Unclassified

2b. GROUP

3. REPORT TITLE

Seasonal Variations of Coastal Currents off the Oregon-Northern California Coast.

4. DESCRIPTIVE NOTES (Type of report and inclusive dates)

Master's Thesis; June, 1972.

5. AUTHOR(S) (First name, middle initial, last name)

ENS William Frederick Whitson, USN

6. REPORT DATE	7a. TOTAL NO. OF PAGES	7b. NO. OF REFS
	52	17

8a. CONTRACT OR GRANT NO.	9a. ORIGINATOR'S REPORT NUMBER(S)
b. PROJECT NO.	
c.	9b. OTHER REPORT NO(S) (Any other numbers that may be assigned this report)
d.	

10. DISTRIBUTION STATEMENT

Approved for public release; distribution unlimited.

11. SUPPLEMENTARY NOTES	12. SPONSORING MILITARY ACTIVITY
	Naval Postgraduate School Monterey, California 93940

13. ABSTRACT

Seasonal longshore flow patterns are examined at four points along the Oregon-Northern California coast. Summer and winter activity is examined as far seaward as 25 nautical miles and as deep as 200 meters. Long-term mean hydrographic data are used to determine geostrophic velocities. A nearshore baroclinic southward flow (~20 cm/sec) is observed at each of the points during the summer. Winter currents are generally very small (<10 cm/sec) and largely barotropic in nature. Seasonal volume transports are presented; corrected velocity profiles are also presented based on data from moored current meters. Qualitative explanations of the observed phenomena are considered.

DD FORM 1 NOV 65 1473 (PAGE 1)

S/N 0101-807-6811

Security Classification

A-31408

KEY WORDS	LINK A		LINK B		LINK C	
	ROLE	WT	ROLE	WT	ROLE	WT
GEOSTROPHY IN SHALLOW WATER						
COASTAL CURRENTS						
UPWELLING						
EAST PACIFIC REGION						
SEASONAL CURRENTS						

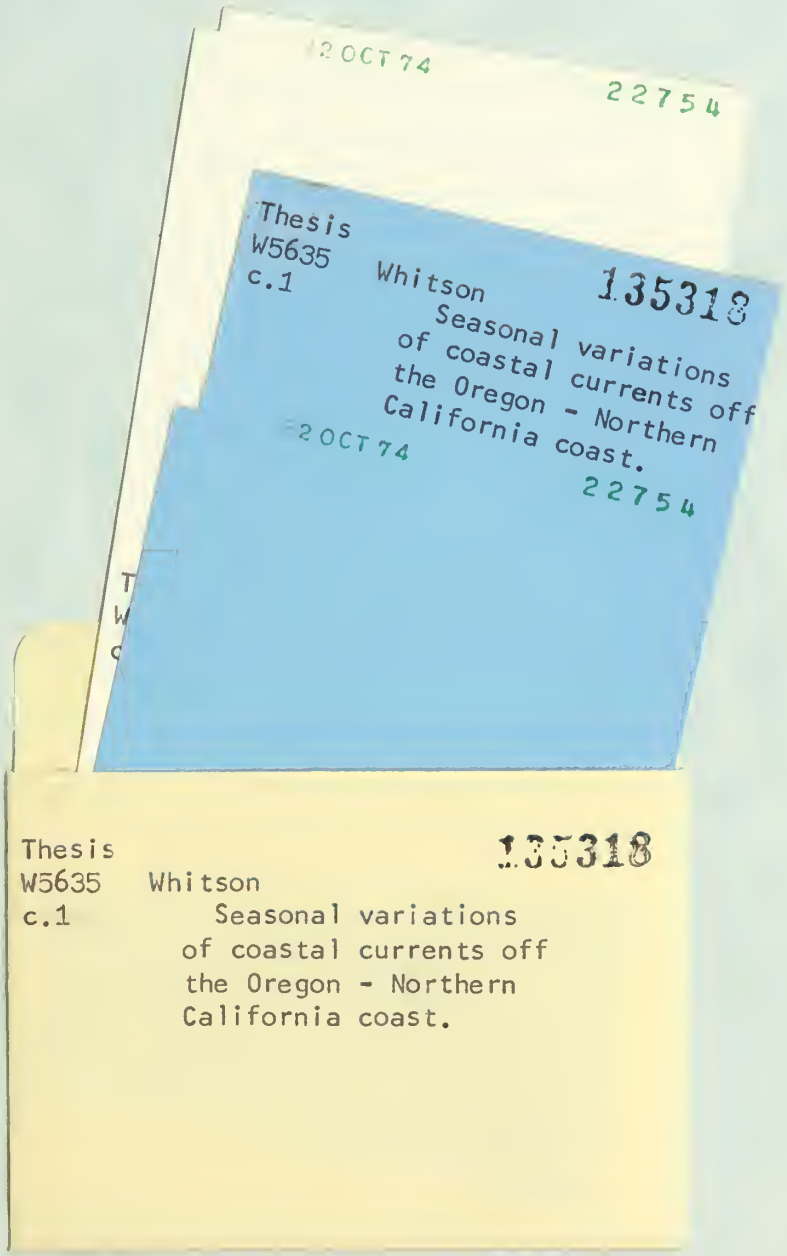
12 OCT 74
22754
Thesis
W5635
c.1
Whitson
Seasonal variations
of coastal currents off
the Oregon - Northern
California coast.
135318
12 OCT 74
22754
Thesis
W5635
c.1
Whitson
Seasonal variations
of coastal currents off
the Oregon - Northern
California coast.
135318

thesW5635
Seasonal variations of coastal currents
3 2768 001 95090 0
DUDLEY KNOX LIBRARY